

A highly conserved gene locus in endofungal bacteria codes for the biosynthesis of symbiosis-specific cyclopeptides

Sarah P. Niehs^{a,1}, Kirstin Scherlach^{a,1}, Benjamin Dose^a, Zerrin Uzum^a, Timothy P. Stinear^b, Sacha J. Pidot^b and Christian Hertweck^{a,c,*}

^aDepartment of Biomolecular Chemistry, Leibniz Institute for Natural Product Research and Infection Biology – Hans Knöll Institute (Leibniz-HKI), Beutenbergstr. 11a, 07745 Jena, Germany

^bDepartment of Microbiology and Immunology, Doherty Institute, University of Melbourne, 792 Elizabeth Street, Melbourne, 3000, Australia

^cFaculty of Biological Sciences, Friedrich Schiller University Jena, 07743 Jena, Germany

*To whom correspondence should be addressed: Email: christian.hertweck@leibniz-hki.de

Edited By: Shibu Yooseph.

Abstract

The tight association of the pathogenic fungus *Rhizopus microsporus* and its toxin-producing, bacterial endosymbionts (*Mycetohabitans* spp.) is distributed worldwide and has significance for agriculture, food production, and human health. Intriguingly, the endofungal bacteria are essential for the propagation of the fungal host. Yet, little is known about chemical mediators fostering the symbiosis, and universal metabolites that support the mutualistic relationship have remained elusive. Here, we describe the discovery of a complex of specialized metabolites produced by endofungal bacteria under symbiotic conditions. Through full genome sequencing and comparative genomics of eight endofungal symbiont strains from geographically distant regions, we discovered a conserved gene locus (*hab*) for a nonribosomal peptide synthetase as a unifying trait. Bioinformatics analyses, targeted gene deletions, and chemical profiling uncovered unprecedented depsipeptides (habitasporins) whose structures were fully elucidated. Computational network analysis and labeling experiments granted insight into the biosynthesis of their nonproteinogenic building blocks (pipecolic acid and β -phenylalanine). Deletion of the *hab* gene locus was shown to impair the ability of the bacteria to enter their fungal host. Our study unveils a common principle of the endosymbiotic lifestyle of *Mycetohabitans* species and expands the repertoire of characterized chemical mediators of a globally occurring mutualistic association.

Keywords: nonribosomal peptides, mutualism, *Mycetohabitans*, *Rhizopus*, sporulation

Significance Statement:

Endosymbiosis is widespread in nature and has been a major driver of eukaryotic evolution. Yet, knowledge about factors that enable the tight association of microorganisms is scarce. We used comparative genomics and chemical analytics to uncover a group of metabolites that mediate the relationship of a globally occurring fungal pathogen and its endosymbiotic bacteria. We show that bacteria dwelling inside *Rhizopus microsporus* universally produce a cyclopeptide complex, describe its biosynthesis, and demonstrate that deletion of the encoding gene cluster impairs the ability of the endobacteria to engage in the mutualistic relationship. Our work uncovers a unique trait of a bacterial–fungal alliance and sheds light on the complex interdependence of microbial partners in endosymbiotic relationships.

Introduction

Endosymbiosis is a special type of symbiosis in which one or more organism(s) dwell within the host's body or cells (1, 2). Such symbioses are the result of millions of years of evolution during which strong and sometimes inseparable bonds have developed between the partners (1, 3). The establishment of such stable symbiotic relationships usually depends on several factors including physical as well as metabolic interactions of the symbiosis partners (4, 5). A persistent association with bacterial endosymbionts is

frequently observed in Mucoromycota hosts (1, 6). An important example is the rice seedling blight fungus *Rhizopus microsporus*, which was shown to host symbiotic bacteria, *Mycetohabitans* spp. strains B1 to B8 (Figure 1A). These endofungal bacteria not only produce virulence-conferring toxins, but also have become essential for the asexual reproduction of the fungus (7). We have identified eight mutualistic *Rhizopus*–*Mycetohabitans* symbioses from environmental samples (8), food contaminants (8), clinical samples (9), and plant pathogens (8). These eight endosymbiotic strains

Competing Interest: The authors declare no competing interest.

¹S.P.N. and K.S. contributed equally to this work.

Received: April 7, 2022. Accepted: August 3, 2022

© The Author(s) 2022. Published by Oxford University Press on behalf of National Academy of Sciences. This is an Open Access article distributed under the terms of the Creative Commons Attribution-NonCommercial-NoDerivs licence (<https://creativecommons.org/licenses/by-nc-nd/4.0/>), which permits non-commercial reproduction and distribution of the work, in any medium, provided the original work is not altered or transformed in any way, and that the work is properly cited. For commercial re-use, please contact journals.permissions@oup.com

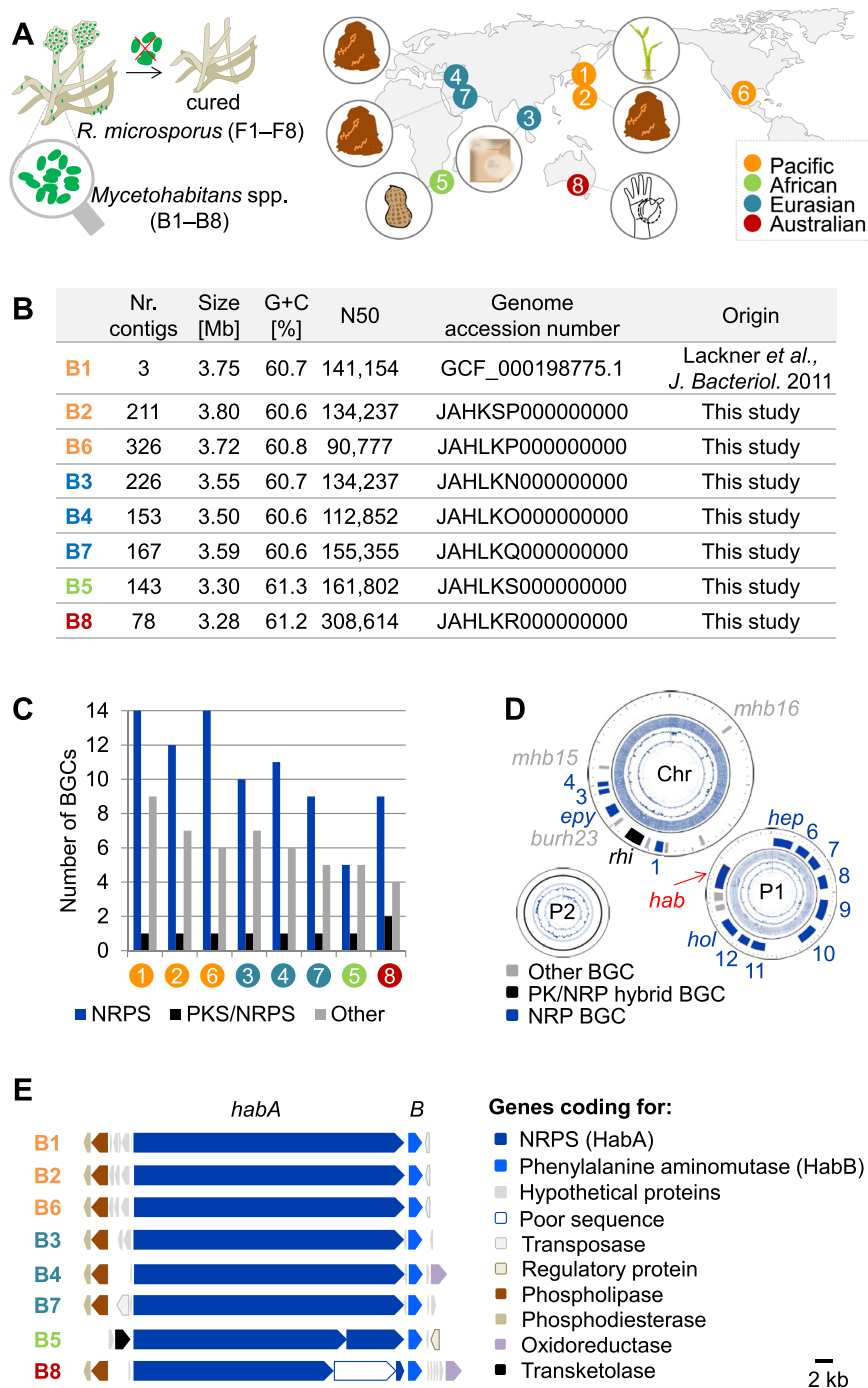


Fig. 1. Survey of the origin of the *Rhizopus* hosts, and orphan biosynthetic gene clusters in their endosymbionts. (A) Global distribution of *Rhizopus*–*Mycetohabitans* symbioses. Isolation background: soil (F2, F4, and F7), necrotic human tissue (F8), nuts (F5), sufu starter culture (F3), rice seedling blight (F1), and unknown (F6). (B) Compilation of genomic features of endosymbiotic strains B1 to B8. (C) Distribution of biosynthetic genes among strains B1 to B8. (D) High biosynthetic potential of *M. rhizoxinica* strain B1. Abbreviations: Chr, chromosome; P1, megaplasmid; P2, plasmid; PK(S), polyketide (synthase); NRP(S), nonribosomal peptide (synthetase); *mhb*, mycetohabin; *burh*, burhizin; *rhi*, rhizoxin; *epy*, endopyrrole; *hol*, holrhizin; and *hep*, heptarhizin BGC. (E) Conserved NRPS genes *habA* and *habB* in the diverse genomic context in all phylogenetically distant branches of endofungal *Mycetohabitans* spp. genomes.

form four geographically and phylogenetically distant clades but appear to have a common ancestor (8) (Figure 1A).

Intriguingly, the fungus lost its ability to sporulate in the absence of the endosymbionts, which is a remarkable control mechanism for the persistence of the symbiosis (10). A number of symbiosis factors were identified such as effectors released by

a type III secretion system (11), TAL effector proteins (12, 13), chitin-degrading enzymes (14), viruses (15), and a specialized O-antigen (16). The strong interdependence of the symbiotic partners is also illustrated by their cooperation in producing the phytotoxic polyketide rhizoxin, the causative agent of rice seedling blight (17–19). The bacterially produced toxin is modified by the

fungus to increase phytotoxic potency (20). Even though the formation of rhizoxin is conserved among all symbionts, the virulence factor is not essential for the establishment of the mutualistic relationship (8).

Genome analyses indicated that the symbiotic bacteria possess a number of gene clusters for specialized metabolism. Yet, besides the rhizoxin complex, no other conserved secondary metabolite has been identified that plays a critical role for the endofungal lifestyle of the symbionts (21–26). The products of various encoded nonribosomal peptide synthetases (NRPSs) have remained cryptic despite extensive screening of *Mycetohabitans* spp. (22–27), thus leaving a gap in our knowledge about chemical mediators at the interface between fungi and bacteria (28).

Here, we report the systematic analysis of *Mycetohabitans* strains by comparative genomics and metabolic profiling, which led to the discovery of cyclic peptides that are conserved in all endosymbionts of *R. microsporus*. We unveil their biosynthetic origin, propose a biosynthesis model and report their critical role in maintaining the bacterial–fungal symbiosis.

Results and discussion

To gain insight into the conserved biosynthetic potential of all eight characterized endofungal strains, we aimed at performing comparative genomics. However, genome sequences of only four *Rhizopus* endosymbionts have been publicly available. These include *Mycetohabitans rhizoxinica* strain B1 (genome accession number: GCF_000198785.1), *Mycetohabitans endofungorum* strain B5 (GCA_002927045.1), and *Mycetohabitans* sp. strains B4 and B7 (GCA_900155955.1 and GCA_900156195.1), of which only the B1 genome sequence is gap-free. Thus, we (re)sequenced the genomes of strains B2 to B8 using the Illumina NextSeq platform.

Comparative genomics shows that all eight bacterial genomes are highly related (Figure S1 and Tables S2–S4). We noted reduced genome sizes (3.3 to 3.8 Mb) characteristic for bacterial endosymbionts, and a reduced G + C content (61%) relative to free-living species (62% to 68%; Figure 1B) (5). By means of antiSMASH v5 (29) and the PKS/NRPS analysis program (30), we investigated the potential for natural product biosynthesis and found that the endofungal bacteria bear a high number of BGCs, mainly encoding NRPSs. The largest number of NRPS genes was found in genomes of members of the Pacific branch, strains B1, B2, and B6 (Figure 1C). Even so, only one NRPS gene locus, likely encoding an octamodular NRPS, (*habA*, 17 kb, accession number: MZ520316) is present in all genome sequences (Figure 1D and E; Tables S6 and S7). This gene locus is highly conserved among the *Rhizopus* endosymbionts (no other orthologues were found in public genome databases) suggesting a potential importance of the gene product for the bacterial–fungal relationship.

To test whether *habA* or encoded products play a role in the symbiotic bacterial–fungal interaction, we aimed at creating a targeted deletion mutant. Since *R. microsporus* is unable to reproduce asexually without the endobacteria (10), sporulation can serve as an indicator of the successful reestablishment of the symbiosis. Thus, the deletion mutant could be examined for its ability to infect the host fungus using a previously described sporulation bioassay (11). Therefore, we generated a knockout construct based on the double-selection plasmid pGL42a (11) and introduced it into *M. rhizoxinica* through electroporation. Gene *habA* was inactivated by integration of a kanamycin resistance cassette in the region that codes for the starter condensation domain (C_S) by a double crossover (11). The successful incorporation of the resis-

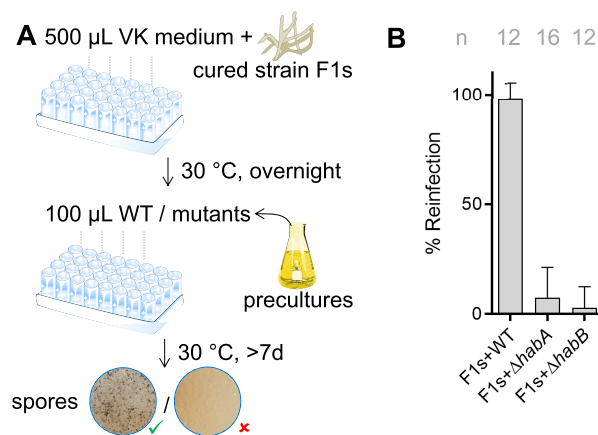


Fig. 2. Evaluation of the biological function of the *hab* gene locus. (A) Schematic view of the reinfection assays. (B) Reinfection events of WT vs. mutant strains for the cured *R. microsporus* (F1s). n, number of biological replicates.

tance marker into the target region (Δ *habA*) was verified by PCR (Figure S8 and Table S10).

To assess the reinfection ability of the *habA* deletion strain, we cured the fungal holobiont from its endosymbiotic bacteria by antibiotic treatment and performed an established sporulation bioassay (Figure 2A; Figure S6) (11). Briefly, the cured *R. microsporus* strain (“F1s”) and either the wild-type strain B1 (WT) or the null mutant Δ *habA* were cocultured and the formation of spores was examined by eye after 7 to 10 days. Whereas, the WT infection experiments showed sporulation rates of 98% ($n = 12$), the mutant was significantly impaired in its ability to induce sporulation of the fungus (8% Δ *habA*, $n = 16$; $P < 0.0001$; Figure 2B). This result unequivocally demonstrates that the *hab* gene locus is critical for the establishment of the symbiotic relationship.

To link the NRPS gene locus to the corresponding secondary metabolite, we first performed computational analyses to predict the product of the encoded assembly line (29, 30). The deduced NRPS HabA consists out of eight modules for chain elongation, and an off-loading thioesterase (TE) domain. We inferred the amino acid sequence of the nonribosomal peptide backbone from the Stachelhaus codes (31) of the adenylation (A) domains in HabA, yet only four positions of the tentative octapeptide could be predicted (X-Val-Thr-X-Ala-Val-X-X; Figure 3A; Figure S4 and Table S5). The presence of three *N*-methyltransferase domains in modules 1, 5, and 7 indicated that three amide groups would be methylated, including the Ala residue (meX-Val-Thr-X-meAla-Val-meX-X).

Directly downstream of *habA* we noted a conserved gene (*habB*) coding for an aminomutase that might play a role in delivering a β -amino acid for the *hab* assembly line (accession number: MZ520317; Figure 1E; Figures S2 and S3) (32). Thus, we scrutinized tentative β -amino acid-activating A domains of the *hab* NRPS by means of a multiple sequence alignment (Figure S3). Specifically, we took into account that β -amino acid-activating A domains often contain bulky aromatic residues (Phe or Tyr in lieu of Ala or Val) adjacent to the Asp that recognizes the β -amino group of the substrate (33). We spotted the conserved D-F/T-motif of β -A domains in HabA-A3. Module 3, however, is predicted to incorporate Thr, which is unlikely to be transformed by an aminomutase (32, 34). Further investigation of the alignment revealed an unusual amino acid sequence inserted upstream of the invariant Asp residue in HabA-A4 and HabA-A8 (19 and 15 amino acids,

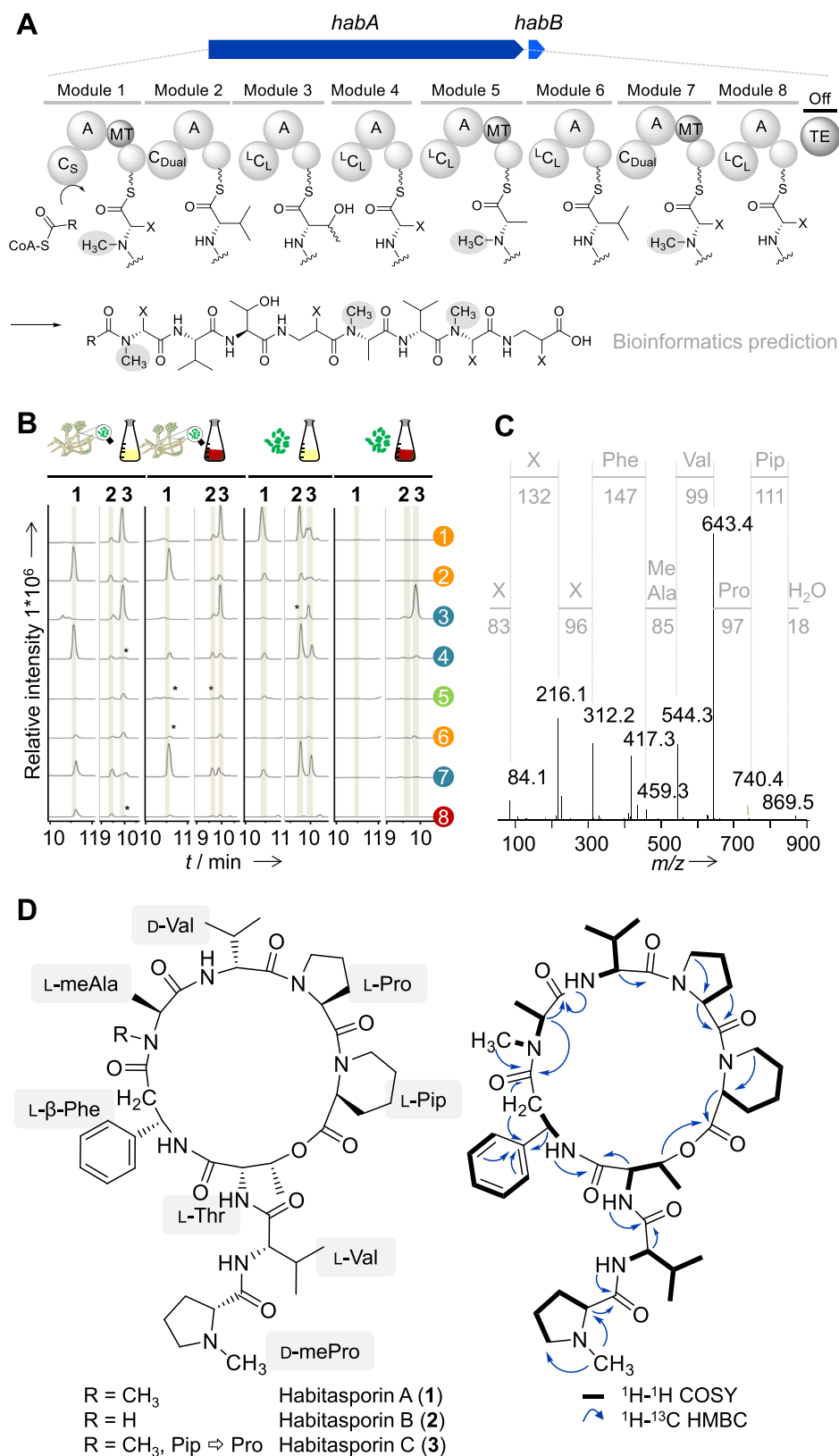


Fig. 3. Identification and structure elucidation of the habitasporins. (A) Bioinformatics prediction of the putative product of the *hab* gene locus. It should be noted that the starter C domain in module 1 is likely inactive as inferred from computational analyses (see Supporting Information). (B) Metabolic profiles of extracts from fungal or bacterial cultures grown in two different media (VK medium, dark red; MGY medium, yellow) as extracted ion chromatograms in positive mode for habitasporin A (**1**; m/z 851.5025 $[M + H]^+$) and B/C (**2** and **3**; m/z 837.4871 $[M + H]^+$). Asterisk, trace amounts. (C) MS/MS fragmentation pattern of base-hydrolyzed **1**. X, elusive amino acid fragment. (D) Structures of habitasporins **1** to **3** with 2D NMR couplings of **1**.

respectively). Based on these results, modules 4 or 8 appeared to be the best candidates for a noncanonical substrate specificity like a β -amino acid (33).

To discover the predicted octapeptide, we investigated and compared the metabolic profiles of all eight axenic bacterial cultures, those of the symbiotic cultures and a culture extract of the $\Delta habA$ deletion strain by HRESI-LC-MS/MS. We evaluated the extracts based on two criteria: (a) specialized metabolites that are produced by all eight WT strains, but not by the deletion mutant, and (b) MS/MS fragmentation patterns that match the bioinformatics prediction meX-Val-Thr-(β)X-meAla-Val-meX-(β)X. We detected three compounds that match both criteria: compound **1** with m/z 851.5025 $[M + H]^+$ ($C_{44}H_{67}N_8O_9$, calculated 851.5026 Da), and compounds **2** and **3**, each with m/z 837.4871 $[M + H]^+$ ($C_{43}H_{65}N_8O_9$, calculated 837.4869 Da; Figure 3B). MS/MS fragmentation experiments of **1** to **3** confirmed that all three compounds are octapeptides (Figure 3C; Figures S9–S12). These metabolites could also be detected in culture extracts of *R. microsporus* strains F1 to F8 containing the endosymbionts. (Figure 3B).

In order to obtain sufficient amounts of pure compounds **1** to **3** for structure elucidation, we optimized various parameters including medium, duration of cultivation, and extraction (Table S1). We screened for the highest production rate among the eight endofungal strains under symbiotic and aposymbiotic conditions through investigation of the resulting extracts by HR-ESI-LC/MS. In this way, the holobiont *Mycetohabitans*–*R. microsporus* CBS 700.68 (strain F7; but not the axenic culture *Mycetohabitans* sp. strain B7) was identified as the most prolific producer. The holobiont was cultivated on TSB agar until complete coverage of the agar plates. Size-exclusion chromatography of the agar extracts, followed by preparative HPLC, yielded pure **1** (1.4 mg), **2** (0.14 mg), and **3** (0.06 mg) per liter agar.

The structures of **1** and **2** were fully elucidated by 1D- and 2D-NMR experiments. The structure of the less abundant derivative **3** was deduced from 1D-NMR data in comparison to **1** (Figure 3D; Figure S15–S29, Tables S11 and S12). Based on ^{13}C and DEPT-135 spectra of **1**, we identified signals for nine carbonyls, 16 methines, 11 methylenes, and eight methyl groups. The 1H spectrum showed three doublets of NH functionalities (δ_H 7 to 9 ppm). Protons resonating at δ_H 4.0 to 5.6 ppm were assigned to CH_α -groups of amino acids. The majority of multiplets (δ_H 1.2 to 2.5 ppm) correspond to methylenes of two proline and one pipercolic acid (Pip). In addition, 1H multiplets at δ_H 7.1 to 7.2 ppm alongside with methine carbon signals at δ_C 126 to 127 ppm pointed to a benzene ring. This aromatic group was identified to be part of the non-proteinogenic amino acid β -phenylalanine (β Phe). In conjunction with MS fragmentations, we deduced the octapeptide backbone as mePro-Val-Thr- β Phe-meAla-Val-Pro-Pip. This finding is surprising because we initially identified a MT domain in module 7, thus expecting a methylated moiety rather than the observed nonmethylated Pro (Figure 3A). ^{13}C , 1H HMBC correlations revealed an ester bond between the Pip and a threonine residue. Consequently, six residues are contained in the cyclopeptide ring, and the remaining two residues constitute a dipeptide tail. The absolute configuration of **1** was determined by derivatization with Marfey's reagent (Table S8) (35).

The structures of **2** and **3** proved to be very similar to **1**. In the proton spectrum of **2**, we observed an additional signal at δ_H 8.7 ppm, which was assigned to the NH-group of alanine. In agreement with MS data, **2** represents a desmethyl congener of **1**. The 1H NMR spectrum of **3**, which lacks signals for Pip, and MS fragmentation data indicate that the Pip moiety is replaced with Pro. We named the octapeptides habitasporins A (**1**), B (**2**), and C (**3**),

reflecting the symbiotic interaction of *Mycetohabitans* species and *R. microsporus* (Figure 3D). With the pure compounds in hand, we attempted to chemically complement the $\Delta habA$ mutant. However, supplementation of the $\Delta habA$ culture with **1** did not restore WT traits under the current experimental setup (Supporting Information). As it is not clear whether **1** (or derivatives) are taken up from the culture broth and how habitasporins are exactly utilized in the bacterial fungal interaction, further complementation approaches did not seem feasible.

Habitasporins represent novel types of cyclopeptides. The NRPs harbor the unusual amino acid residues Pip and β Phe. β Phe was previously found in NRPs as well as macrolactam antibiotics and other molecules (32) including the anticancer agent taxol (36) from plants, the antibiotics andrimid (37, 38) and hitachimycin (39) from Actinobacteria, and β Tyr in the myxobacterial chondramide C (40). β -Amino acids can enhance structural diversity of a natural product and often confer particular bioactivities (32). Yet, in the case of habitasporins, whole-cell bioactivity assays showed no cytotoxic or antimicrobial properties of **1**, whereas congener **2** exhibited weak antifungal activity against *Penicillium notatum* in an agar diffusion assay (Table S9). Furthermore, no phytotoxic effects against three common test strains were observed for **1** (Figure S7).

Besides *habA*, the only other conserved gene in the *hab* BGCs across all eight genomes is *habB* (Figure 1E). A BLAST search (41, 42) suggested that the deduced gene product, HabB, codes for a phenylalanine aminomutase, an enzyme converting α Phe into the β -form (43). To substantiate the function of HabB we constructed a sequence similarity network and a genome neighborhood network using the online tool EFI-EST (Figure 4A; Figure S5) (44, 45). In the sequence similarity network, we noted orthologues from assembly lines for hitachimycin (39), andrimid (37), and chondramide C (40). The associated aminomutases were reported to catalyze the isomerization of α Phe or α Tyr into their β -counterpart. Accordingly, aminomutase HabB would provide the β Phe unit of habitasporins A (**1**) and B (**2**).

To verify the involvement of HabB in the *hab* pathway, we constructed a second mutant ($\Delta habB$) using a selection-enhanced version of the *pheS*-harboring plasmid (24). HPLC-HRMS analysis of the verified $\Delta habB$ mutant showed that its metabolic profile is devoid of **1** to **3** (Figure 4B; Figure S30), thus confirming an essential role of the aminomutase in habitasporin biosynthesis. Habitasporin production in $\Delta habB$ cultures, however, could not be restored by external β Phe supplementation. *Mycetohabitans rhizoxinica* might be missing specific β -amino acid transporters responsible for uptake of β Phe from the medium (46). To further support our observation that the *hab* gene locus plays an essential role in the establishment of the symbiotic relationship, we tested the reinfection ability of the $\Delta habB$ mutant applying the sporulation assay. As observed for the $\Delta habA$ mutant, the $\Delta habB$ deletion strain shows a significantly reduced ability to induce sporulation of the fungus (3% $\Delta habB$, $n = 12$; $P < 0.0001$; Figure 2B).

Pip residues—as observed in habitasporins—are even less common than β -amino acids. Pip was shown to be part of only a small number of secondary metabolites isolated from Actinobacteria, plants and fungi (Figure 4C) (47, 48). In total, three main biosynthetic pathways have been described for Pip assembly: the Δ^1 -piperideine-6-carboxylate (P6C), Δ^1 -piperideine-2-carboxylate (P2C), and the cyclodeaminase routes (Figure 4C) (49). Bacteria were shown to biosynthesize Pip through all three pathways. Cyclodeaminases are the most commonly observed Pip-forming enzymes in bacterial NRP formation (rapamycin, **4** (50) and virginamycin, **5** (51)). The P2C pathway was described for plants

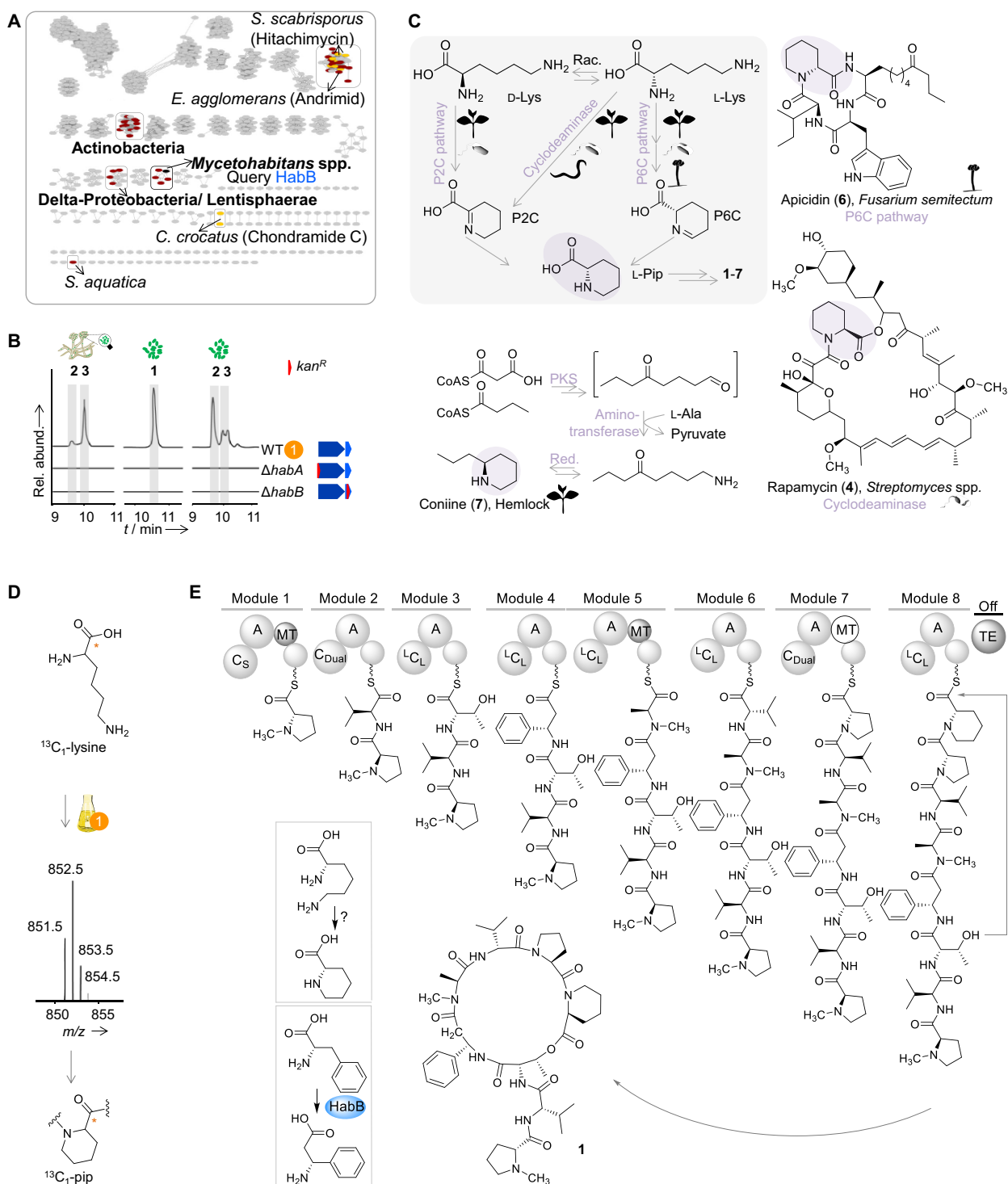


Fig. 4. Biosynthetic origin of habitasporins. (A) Sequence similarity network using HabB sequence reveals distribution of aminomutases encoded in known (yellow nodes), uncharacterized BGCs (red nodes), and other genes (gray). (B) Metabolic profiles of bacteria *M. rhizoxinica* HK1454 or fungus *R. microsporus* ATCC62417 as WT or deletion mutants. Extracted ion chromatograms of **1** (m/z 851.5025 [$M + H$]⁺) or **2** and **3** (m/z 837.4871 [$M + H$]⁺) are displayed. *kan^R*, kanamycin resistance cassette. (C) Selected natural products harboring a Pip moiety, their producing organisms, and the biosynthesis of Pip (in purple). P2C, Δ^1 -piperideine-2-carboxylate. (D) Mass shift (m/z +1 Da) observed in isotopic pattern of **1** after supplementing a *M. rhizoxinica* culture with ¹³C₁-lysine. (E) Biosynthetic model showing the assembly of **1** in Hab. Nonfunctional domain in white.

as well as for *Pseudomonas* spp. (49). In fungi, dedicated reductases in the P6C pathway were described for apicidin (**6**) formation (52). Pip moieties can also be produced by polyketide synthases in combination with aminotransferases in a nonenzymatic

cyclization reaction in plants, e.g. for coniine (**7**, 47). We mined the genome sequence of *Mycetohabitans* spp. strains B1 to B8 for genes coding for enzymes required for the P6C, P2C, and cyclodeaminase pathways (49). However, no homologues of genes coding for

cyclodeaminases, dedicated reductases, dehydrogenases, and aminotransferases could be identified.

As the Pip moiety is commonly derived from lysine, we performed stable-isotope labeling experiments by adding $^{13}\text{C}_1$ -lysine to the culture broth of *M. rhizoxinica*. LC-HR-MS analyses revealed a mass shift ($m/z +1$ Da) in the isotopic pattern of **1** (Figure 4D). By comparing the MS/MS spectra of labeled and unlabeled **1**, we observed exclusive ^{13}C labeling of the C_α of the Pip residue (Figures S13 and S14). The absence of a dedicated gene coding for Pip formation has been reported for the BGC of the neuroprotective meridamycin (53). It was also shown that a cyclodeaminase mutant of the rapamycin producer still generated minor amounts of the Pip-bearing metabolite (50). Thus, it appears that the lack of dedicated Pip genes in BGCs can be compensated by alternative routes for Pip formation in bacteria (Figure 4C) (48, 49).

On the basis of the bioinformatic, genetic and isotope labeling experiments, we propose a model for habitasporin assembly (Figure 4E). The nonproteinogenic amino acid Pip is formed by an elusive protein, whereas the phenylalanine aminomutase HabB is responsible for β Phe production. The NRPS architecture is largely colinear with the octapeptide backbone. *N*-methyltransferase domains in modules 1 and 5 catalyze the methylation of the first proline and alanine residues. A third *N*-methyltransferase in module 7 appears to be nonfunctional as *N*-methylation cannot take place at the other proline amide. Eventually, the linear peptide is cyclized by the TE domain, forming an ester bond between the hydroxy group of Thr (loaded by HabA-A3) and the carboxy moiety of the last residue, Pip (Figure 4E). Based on the peptide structure and the colinearity rule, HabA-A4 (but not HabA-A3) incorporates the β Phe moiety. This finding is contrary to the D-F/T-motif prediction (Figure S3). Other exceptions are known (e.g. AdmJ (54) and CmdD (40)), yet the identified insertion of 19 amino acids in HabA-A4 might indicate another mode of recognition in the β -A domains than previously proposed (33).

Besides the rhizoxin complex, habitasporins represent the only identified specialized metabolites that are synthesized by all characterized endofungal *Mycetohabitans* strains. The encoding gene locus (*hab*) is the first characterized secondary metabolite biosynthetic gene cluster that is critical for the establishment of the bacterial–fungal symbiosis. The discovery of habitasporins as a common metabolic principle of endosymbiotic bacteria of *R. microsporus* further extends the repertoire of identified chemical mediators of mutualistic microbial interaction and provides additional insight into the complex regulatory system of a unique, yet globally occurring bacterial–fungal symbiosis.

Materials and Methods

A full materials and methods section is provided as supplemental information.

Acknowledgments

We thank H.-M. Dahse and C. Weigel for the bioactivity testing, B. Urbansky for the technical assistance, A. Perner for the MS measurements, and H. Heinecke for the NMR measurements. Support by S. Richter and S. Schieferdecker is gratefully acknowledged.

Supplementary Material

Supplementary material is available at [PNAS Nexus](#) online.

Funding

Z.U. was funded by the Jena School for Microbial Communication (JSMC). S.P.N. was funded by the Deutsche Forschungsgemeinschaft (DFG, German Research Foundation)—Project-ID 239748522–SFB 1127, and by the Leibniz Award (to C.H.).

Authors' Contributions

S.P.N., K.S., and B.D. designed and performed the research, analyzed data, and wrote the paper. Z.U., T.P.S., and S.J.P. performed the research and analyzed data. C.H. designed the research and wrote the paper.

Data Availability

All data are included in the manuscript and/or supporting information.

References

1. Pawlowska TE, et al. 2018. Biology of fungi and their bacterial endosymbionts. *Annu Rev Phytopathol.* 56:289–309.
2. Wernegreen JJ. 2012. Endosymbiosis. *Curr Biol.* 22:R555–R561.
3. Nygaard S, et al. 2016. Reciprocal genomic evolution in the ant-fungus agricultural symbiosis. *Nat Commun.* 7:1–9.
4. Hentschel U, Steinert M, Hacker J. 2000. Common molecular mechanisms of symbiosis and pathogenesis. *Trends Microbiol.* 8:226–231.
5. Moran NA, Wernegreen JJ. 2000. Lifestyle evolution in symbiotic bacteria: insights from genomics. *Trends Ecol Evol.* 15:321–326.
6. Bonfante P, Desirò A. 2017. Who lives in a fungus? The diversity, origins and functions of fungal endobacteria living in *Mucoromycota*. *ISME J.* 11:1727–1735.
7. Estrada-de los Santos P, et al. 2018. Whole genome analyses suggests that *Burkholderia sensu lato* contains two additional novel genera (*Mycetohabitans* gen. nov., and *Trinickia* gen. nov.): implications for the evolution of diazotrophy and nodulation in the Burkholderiaceae. *Genes.* 9:389.
8. Lackner G, et al. 2009. Global distribution and evolution of a toxigenic *Burkholderia-Rhizopus* symbiosis. *Appl Environ Microbiol.* 75:2982–2986.
9. Kerr PC, Turner H, Davidson A, Bennett C, Maslen M. 1988. Zygomycosis requiring amputation of the hand: an isolated case in a patient receiving haemodialysis. *Med J Aust.* 148:258–259.
10. Partida-Martinez LP, Monajembashi S, Greulich K-O, Hertweck C. 2007. Endosymbiont-dependent host reproduction maintains bacterial–fungal mutualism. *Curr Biol.* 17:773–777.
11. Lackner G, Moebius N, Hertweck C. 2011. Endofungal bacterium controls its host by an *hrp* type III secretion system. *ISME J.* 5: 252.
12. Richter I, et al. 2020. Secreted TAL effectors protect symbiotic bacteria from entrapment within fungal hyphae. *bioRxiv*. DOI: 10.1101/2020.03.28.013177.
13. Carter ME, et al. 2020. A TAL effector-like protein of an endofungal bacterium increases the stress tolerance and alters the transcriptome of the host. *Proc Natl Acad Sci.* 117:17122–17129.
14. Moebius N, Üzümlü Z, Dijksterhuis J, Lackner G, Hertweck C. 2014. Active invasion of bacteria into living fungal cells. *eLife.* 3:e03007.
15. Espino-Vázquez AN, et al. 2020. Narnaviruses: novel players in fungal–bacterial symbioses. *ISME J.* 14:1743–1754.

16. Leone MR, et al. 2010. An unusual galactofuranose lipopolysaccharide that ensures the intracellular survival of toxin-producing bacteria in their fungal host. *Angew Chem Int Ed*. 49:7476–7480.
17. Sato Z, et al. 1983. Studies on rhizoxin, a phytotoxin produced by *Rhizopus chinensis* causing rice seedling blight. *Ann Phytopathol Soc Jpn*. 49:128.
18. Takahashi M, et al. 1987. Rhizoxin binding to tubulin at the maytansine-binding site. *Biochim Biophys Acta Gen Sub*. 926:215–223.
19. Partida-Martinez LP, Hertweck C. 2005. Pathogenic fungus harbours endosymbiotic bacteria for toxin production. *Nature*. 437:884–888.
20. Scherlach K, Busch B, Lackner G, Paszkowski U, Hertweck C. 2012. Symbiotic cooperation in the biosynthesis of a phytotoxin. *Angew Chem Int Ed*. 51:9615–9618.
21. Lackner G, Moebius N, Partida-Martinez LP, Boland S, Hertweck C. 2012. Evolution of an endofungal lifestyle: deductions from the *Burkholderia rhizoxinica* genome. *BMC Genomics*. 12:210.
22. Niehs SP, Dose B, Scherlach K, Roth M, Hertweck C. 2018. Genomics-driven discovery of a symbiont-specific cyclopeptide from bacteria residing in the rice seedling blight fungus. *ChemBioChem*. 19:2167–2172.
23. Niehs SP, Scherlach K, Hertweck C. 2018. Genomics-driven discovery of a linear lipopeptide promoting host colonization by endofungal bacteria. *Org Biomol Chem*. 16:8345–8352.
24. Niehs SP, et al. 2019. Genome mining reveals endopyrroles from a nonribosomal peptide assembly line triggered in fungal-bacterial symbiosis. *ACS Chem Biol*. 14:1811–1818.
25. Niehs SP, et al. 2020. Mining symbionts of spider-transmitted fungus illuminates uncharted biosynthetic pathways to cytotoxic benzolactones. *Angew Chem Int Ed*. 59:7766–7771.
26. Partida-Martinez LP, et al. 2007. Rhizonin, the first mycotoxin isolated from the zygomycota, is not a fungal metabolite but is produced by bacterial endosymbionts. *Appl Environ Microbiol*. 73:793–797.
27. Bratovanov EV, et al. 2019. Genome mining and heterologous expression reveal two distinct families of lasso peptides highly conserved in endofungal bacteria. *ACS Chem Biol*. 15:1169–1176.
28. Scherlach K, Hertweck C. 2020. Chemical mediators at the bacterial-fungal interface. *Annu Rev Microbiol*. 74:267–290.
29. Blin K, et al. 2019. antiSMASH 5.0: updates to the secondary metabolite genome mining pipeline. *Nucleic Acids Res*. 47:W81–W87.
30. Bachmann BO, Ravel J. 2009. Methods for *in silico* prediction of microbial polyketide and nonribosomal peptide biosynthetic pathways from DNA sequence data. *Methods Enzymol*. 458:181–217.
31. Stachelhaus T, Mootz HD, Marahiel MA. 1999. The specificity-conferring code of adenylation domains in nonribosomal peptide synthetases. *Chem Biol*. 6:493–505.
32. Kudo F, Miyanaga A, Eguchi T. 2014. Biosynthesis of natural products containing β -amino acids. *Nat Prod Rep*. 31:1056–1073.
33. Miyanaga A, Cieślak J, Shinohara Y, Kudo F, Eguchi T. 2014. The crystal structure of the adenylation enzyme VinN reveals a unique β -amino acid recognition mechanism. *J Biol Chem*. 289:31448–31457.
34. Wu B, Szymański W, Heberling MM, Feringa BL, Janssen DB. 2011. Aminomutases: mechanistic diversity, biotechnological applications and future perspectives. *Trends Biotechnol*. 29:352–362.
35. Bhushan R, Brückner H. 2011. Use of Marfey's reagent and analogs for chiral amino acid analysis: assessment and applications to natural products and biological systems. *J Chromatogr B*. 879:3148–3161.
36. Walker KD, Klettke K, Akiyama T, Croteau R. 2004. Cloning, heterologous expression, and characterization of a phenylalanine aminomutase involved in taxol biosynthesis. *J Biol Chem*. 279:53947–53954.
37. Jin M, Fischbach MA, Clardy J. 2006. A biosynthetic gene cluster for the acetyl-CoA carboxylase inhibitor andrimid. *J Am Chem Soc*. 128:10660–10661.
38. Fredenhagen A, et al. 1987. Andrimid, a new peptide antibiotic produced by an intracellular bacterial symbiont isolated from a brown planthopper. *J Am Chem Soc*. 109:4409–4411.
39. Kudo F, et al. 2015. Genome mining of the hitachimycin biosynthetic gene cluster: involvement of a phenylalanine-2,3-aminomutase in biosynthesis. *ChemBioChem*. 16:909–914.
40. Rachid S, Krug D, Weissman KJ, Müller R. 2007. Biosynthesis of (R)- β -tyrosine and its incorporation into the highly cytotoxic chondramides produced by *Chondromyces crocatus*. *J Biol Chem*. 282:21810–21817.
41. Altschul SF, Gish W, Miller W, Myers EW, Lipman DJ. 1990. Basic local alignment search tool. *J Mol Biol*. 215:403–410.
42. Camacho C, et al. 2009. BLAST+: architecture and applications. *BMC Bioinf*. 10:421.
43. Chesters C, Wilding M, Goodall M, Micklefield J. 2012. Thermal bifunctionality of bacterial phenylalanine aminomutase and ammonia lyase enzymes. *Angew Chem Int Ed*. 51:4344–4348.
44. Gerlt JA, et al. 2015. Enzyme function initiative-enzyme similarity tool (EFI-EST): a web tool for generating protein sequence similarity networks. *Biochim Biophys Acta Proteins Proteomics*. 1854:1019–1037.
45. Zallot R, Oberg NO, Gerlt JA. 2018. 'Democratized' genomic enzymology web tools for functional assignment. *Curr Opin Chem Biol*. 47:77–85.
46. Schneider F, Krämer R, Burkovski A. 2004. Identification and characterization of the main β -alanine uptake system in *Escherichia coli*. *Appl Microbiol Biotechnol*. 65:576–582.
47. Hotti H, Rischer H. 2017. The killer of Socrates: coniine and related alkaloids in the plant kingdom. *Molecules*. 22:1962.
48. He M. 2006. Pipecolic acid in microbes: biosynthetic routes and enzymes. *J Ind Microbiol Biotechnol*. 33:401–407.
49. Vranova V, Lojkova L, Rejsek K, Formanek P. 2013. Significance of the natural occurrence of L-versus D-pipecolic acid: a review. *Chirality*. 25:823–831.
50. Gatto GJ, Boyne MT, Kelleher NL, Walsh CT. 2006. Biosynthesis of pipecolic acid by RapL, a lysine cyclodeaminase encoded in the rapamycin gene cluster. *J Am Chem Soc*. 128:3838–3847.
51. Pulsawat N, Kitani S, Nihira T. 2007. Characterization of biosynthetic gene cluster for the production of virginiamycin M, a streptogramin type A antibiotic, in *Streptomyces virginiae*. *Gene*. 393:31–42.
52. Jin JM, et al. 2010. Functional characterization and manipulation of the apicidin biosynthetic pathway in *Fusarium semitectum*. *Mol Microbiol*. 76:456–466.
53. Jiang H, et al. 2011. Investigation of the biosynthesis of the pipecolate moiety of neuroprotective polyketide meridamycin. *J Antibiot*. 64:533.
54. Fortin PD, Walsh CT, Magarvey NA. 2007. A transglutaminase homologue as a condensation catalyst in antibiotic assembly lines. *Nature*. 448:824–827.